# Fabrication of Graphene/Polyaniline Composite Paper *via In Situ* Anodic Electropolymerization for High-Performance Flexible Electrode

**Da-Wei Wang,[†,‡,§] Feng Li,[†,*] Jinping Zhao,[†] Wencai Ren,[†] Zhi-Gang Chen,[†] Jun Tan,[†] Zhong-Shuai Wu,[†] Ian Gentle,[‡,§] Gao Qing Lu,[‡] and Hui-Ming Cheng[†,*]**

[†]Shenyang National Laboratory for Materials Science Institute of Metal Research, Chinese Academy of Sciences, 72 Wenhua Road, Shenyang 110016, China, [‡]Australian Research Council Centre of Excellence for Functional Nanomaterials, AIBN, and [§]School of Chemistry and Molecular Biosciences, The University of Queensland, Brisbane, Qld 4072, Australia



**ABSTRACT** Freestanding and flexible graphene/polyaniline composite paper was prepared by an *in situ* anodic electropolymerization of polyaniline film on graphene paper. This graphene-based composite paper electrode, consisting of graphene/polyaniline composite sheets as building blocks, shows a favorable tensile strength of 12.6 MPa and a stable large electrochemical capacitance (233 F $g^{-1}$ and 135 F $cm^{-3}$ for gravimetric and volumetric capacitances), which outperforms many other currently available carbon-based flexible electrodes and is hence particularly promising for flexible supercapacitors.

**KEYWORDS:** graphene · polyaniline · electrode · supercapacitor

Flexible energy storage devices[1−3] have many potential applications in portable electronic devices,[4−6] including roll-up display, electronic paper, stretchable integrated circuits, and wearable systems for personal multimedia, computing, or medical devices. Flexible supercapacitors are available with large power density, moderate energy density, good operational safety, and long cycling life and hence are highly desirable as a modern energy storage system.[7] A freestanding binder-free electrode with favorable mechanical strength and large capacitance is a vital component of a flexible supercapacitor. Although transition metal oxides and conducting polymers have been widely studied as supercapacitor electrode materials, only carbon-based materials have shown favorable flexibility and hence been promising as freestanding soft electrodes. Papers, films, and/or clothes made from carbon nanotubes/fibers have been demonstrated to be suitable as freestanding electrodes.[2,8−13] Nevertheless, the less active surface of carbon materials always prevents them from high capacitance performance. The incorporation of an electrochemically active second phase in a carbon-based freestanding electrode can dramatically enhance the electrode capacitance.[14]

Graphene is an intriguing two-dimensional carbon material and has attracted much research attention due to several breakthroughs in fundamental research and promising practical applications.[15−30] Chemical modified graphene exhibits enormous active edges and oxygen functional groups. It has extraordinary electrochemical and mechanical properties comparable to or even better than carbon nanotubes.[21,26,27] Flexible papers with graphene sheet or graphene oxide sheet as sole building block have already been fabricated by flow-directed assembly.[16,25,31,32] Graphene paper presents excellent tensile modulus up to 35 GPa and room temperature electrical conductivity of 7200 S $m^{-1}$.[25] These intriguing characteristics enable graphene paper as a freestanding electrode. Various conducting polymers have been widely studied as electrode materials for supercapacitors because of their high capacitance, easy production, and low cost. However, poor conductivity and weak flexibility of conducting polymers limit them from usage in high-performance flexible supercapacitors. It has been confirmed that graphene can enhance not only the electric conductivity of silica[18] but especially the mechanical strength of polymer composites.[21] This work is aimed to prepare graphene-conducting polymer composite paper as a flexible electrode combining the advantages of graphene paper (high

*Address correspondence to cheng@imr.ac.cn, fli@imr.ac.cn.

Received for review March 25, 2009 and accepted May 25, 2009.

**Published online June 2, 2009.**
**10.1021/nn900297m CCC: $40.75**

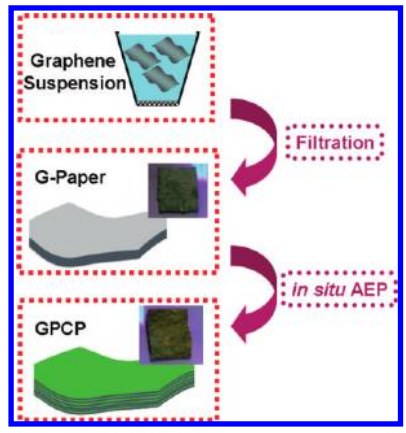


**Figure 1. Illustrative fabrication process toward GPCP.**

conductivity and flexibility) and conducting polymer (large capacitance). Polyaniline (PANi) is a common conducting polymer[33] and is generally considered to promote the electrochemical capacitance of carbon materials.[7] For instance, PANi modified carbon monolith and mesoporous carbon showed significantly improved capacitance.[34,35] Therefore, the inclusion of PANi is expected to maximize the unique potential of graphene paper as a freestanding electrode for a flexible supercapacitor.

In this work, we demonstrate the preparation of a graphene/polyaniline composite paper (GPCP) by *in situ* anodic electropolymerization (AEP) of aniline monomers into a PANi film on graphene paper (G-paper). This composite paper combines flexibility, conductivity, and electrochemical activity and exhibits excellent gravimetric capacitance of 233 F $g^{-1}$ and volumetric capacitance of 135 F $cm^{-3}$, outperforming many other currently available carbon-based freestanding electrodes.

## RESULTS AND DISCUSSION

Attentive formation of the hybrid paper having both highly conductive and flexible graphene and large storage capacity polyaniline will lead to a soft electrode with enhanced large capacitance. The fabrication of GPCP essentially includes two steps as illustrated in Figure 1: (1) directional flow guided assembly of graphene paper (G-paper) by vacuum infiltration, and (2) *in situ* AEP of aniline giving GPCP. In a typical process, vacuum infiltration of graphene suspension through a cellulose membrane yielded, after vacuum drying, a flexible black G-paper (Figure 2). The flow-directed assembly results in a layered structure of G-paper with graphene sheets as building blocks.[25,31] GPCP was prepared by performing AEP on a G-paper electrode impregnated in 200 mL solution containing 0.05 M aniline and 0.5 M $H_2SO_4$, as shown in Figure 3A. The potential of G-paper was linearly shifted from open circuit potential to 0.75 V *versus* a saturated calomel reference electrode (SCE) at a rate of 10 mV $s^{-1}$ and then kept constant during which the current changes as the time prolonged (Figure 3B). In this procedure, the adsorbed aniline monomers on the surface of graphene sheets will be electropolymerized to form PANi between the layers of neighboring graphene sheet layers. The similar morphology of GPCP to G-paper implies that the composite paper electrode maintains the layered structure (digital photos in Figure 1). Raman spectroscopy was used to study the surface compositions of G-paper and GPCP-60s/300s/900s, where xs denotes the AEP time (Figure 4). Two new representative peaks arising from PANi can be indexed at 1167 and 1468 $cm^{-1}$, apart from the D/G bands of graphene paper, which correspond to C−H vibrations in quinoid/phenyl groups and semiquinone radical cation structure in PANi, respectively.[36−39] The intensities of Raman peaks associated with PANi were increased as AEP continued, indicating the gradual aggregation of PANi. Thus GPCP electrodes with variable mechanical and electrochemical properties can be accessible by simply adjusting the AEP time. The success of GPCP preparation can result in a soft composite electrode having (i) the improved

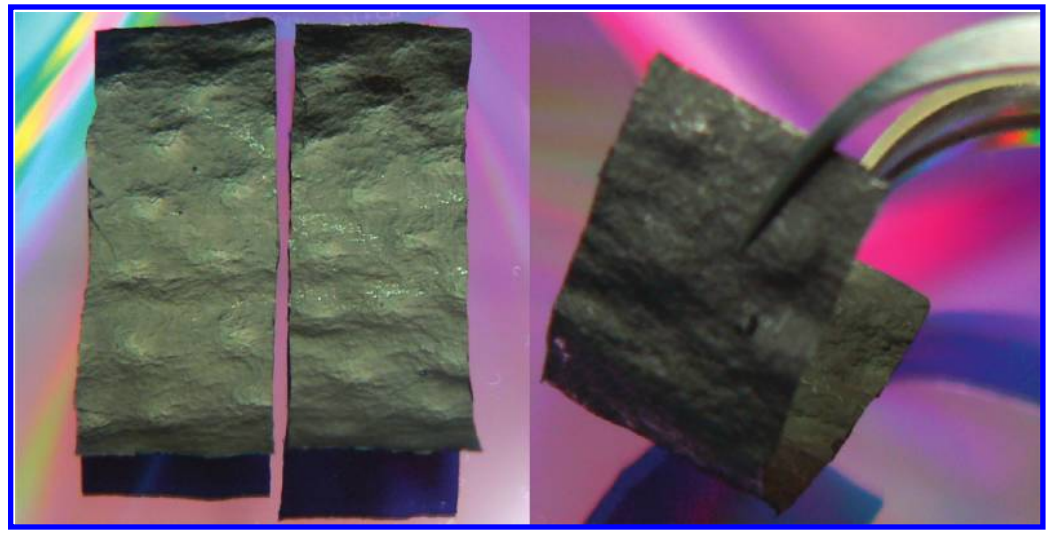

**Figure 2. Digital camera images of (left) two freestanding G-papers (30 mm × 10 mm) and (right) a flexible G-paper.**

electric conductivity of PANi due to the existence of graphene, (ii) homogeneous ion accessibility and high interfacial charge uptake inside the layered structure of GPCP, and (iii) a triple supercapacitive storage mechanism (electric double layer charging/discharging and pseudocapacitive redox reactions of oxygen functional groups of graphene sheets layers and pseudocapacitive redox reactions of PANi layers).

Scanning electron microscope (SEM) images of the G-paper and GPCP-900s are shown in Figure 5A−D. The GPCP-900s inherits the layer-by-layer structure of the G-paper but in a denser stacking (Figure 5A,B). This structural compression after AEP treatment was also detected by liquid nitrogen cryo-sorption analysis. The Brunauer−Emmett−Teller (BET) specific surface areas (SSA) of the G-paper and GPCP-900s are 94 and 39 $m^2 g^{-1}$, respectively. The densely packed graphene/PANi sheets in GPCP-900s are attributed to the electrode assembly/capillary hydrostatic pressures during AEP treatment in solution and the voids replaced by PANi. The enhanced interlayer connection can improve the mechanical property of GPCP-900s, as shown later. High-magnification SEM images (Figure 5C,D) indicate that the graphene/PANi sheets in GPCP-900s exhibit a similar morphology to the pristine graphene sheets in G-paper. Transmission electron microscope (TEM) images further confirm their similarity (Figure 5E,F), without particulate or whisker-like PANi nanostructures.[34,35] Before AEP, the pristine graphene sheets in G-paper are nearly transparent under electron irradiation and have much smaller contrast than that of amorphous carbon film (thickness ~ 100 nm) supported on a copper grid. These features were rarely changed after AEP, implying the coating of an extremely thin PANi film on graphene sheets in GPCP-900s. This film-like surface plating is quite distinct from the formation of PANi nanoparticles

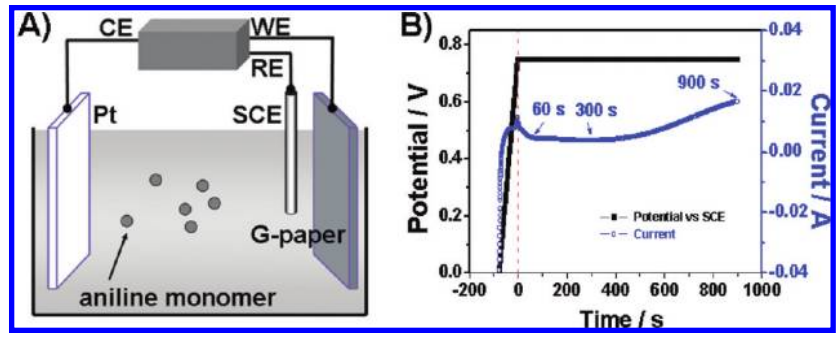


**Figure 3. (A) Cartoon illustrating the AEP of aniline monomer on G-paper, (B) the potential and current response recorded during PANi electropolymerization on G-paper. CE: counter electrode (Pt plate). WE: working electrode (G-paper). RE: reference electrode (SCE).**

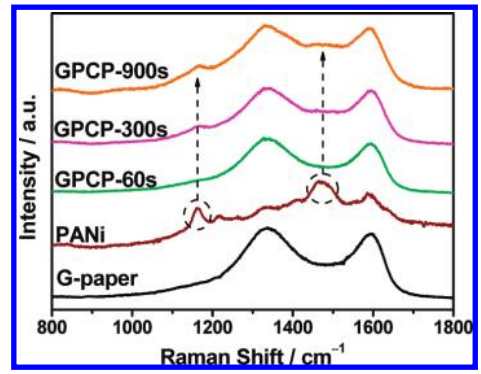


**Figure 4. Raman spectra of the G-paper, PANi, and GPCP-60s/300s/900s.**

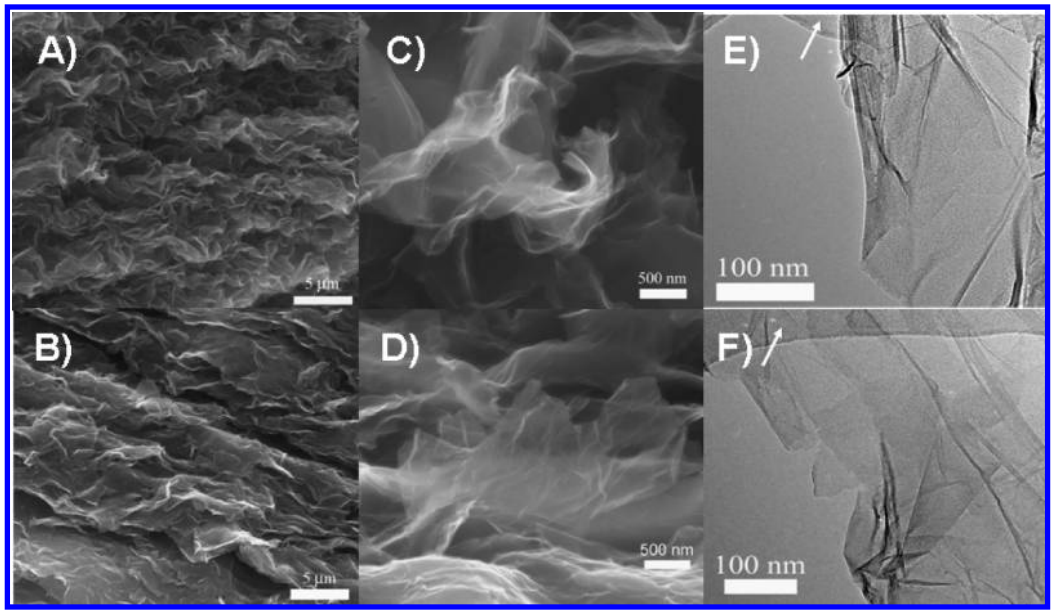


**Figure 5. SEM and TEM images of the G-paper (A,C,E) and GPCP-900s (B,D,F). (A,B) Low-magnification SEM images, showing the stacked layer-by-layer structure. (C,D) High-magnification SEM images and (E,F) low-magnification TEM images, showing the morphology of graphene and graphene/PANi sheets. Arrows in panels E and F denote the amorphous carbon film deposited on the copper grid.**

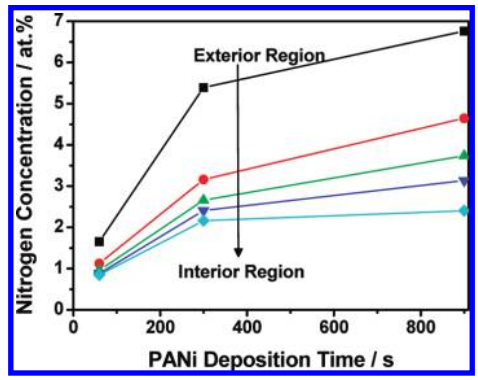


**Figure 6. XPS depth distribution of nitrogen in GPCP paper with different AEP time.**

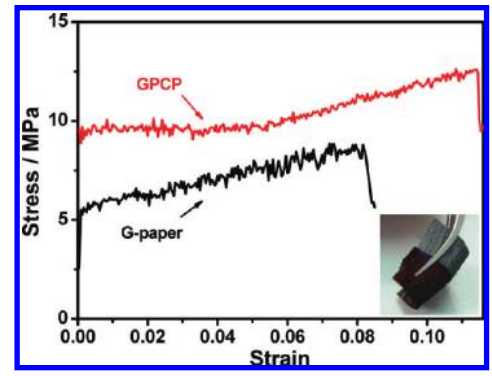


**Figure 8. Mechanical stress−strain curves of the G-paper and GPCP-900s. Inset is the flexible G-paper (top) and GPCP-900s (bottom).**

in a hierarchical porous carbon monolith.[35] Interestingly, the featureless PANi film on a nonporous carbon monolith with a flat surface is comparable with our results.[35]

The distribution of polyaniline in GPCP actually involves (1) the three-dimensional distribution of polyaniline on the exterior and inner part of the GPCP paper and (2) the two-dimensional distribution of polyaniline on the surface of individual graphene sheet as a building block of the GPCP paper. To reveal the 3D distribution of polyaniline in GPCP, we adopted the X-ray photoelectron spectroscopy (XPS) analysis coupled with a depth distribution to detect the nitrogen concentration, as a clue for the polyaniline amount in 3D GPCP paper. From Figure 6, we can easily read two implications: (1) the polyaniline amount decreases from the outer surface to inner surface of GPCP, which is independent of the AEP period; (2) as the deposition time increases, the polyaniline amount increases, which is independent of the location in the 3D GPCP. Electron energy loss spectroscopy (EELS) was used to establish the distribution of PANi film on the surface of an individual graphene/polyaniline sheet by detecting nitrogen signals from PANi. A bright field TEM and the corresponding EELS elements (N, C, and O) mapping images are displayed in Figure 7. The uniform distribution of nitrogen along with carbon and oxygen over the whole area of graphene/PANi sheet suggests the presence of a homogeneous ultrathin PANi film on an individual graphene sheet. The above results suggest that, although the distribution of polyaniline on individual 2D graphene sheet is homogeneous, its distribution is inhomogeneous in the 3D structure of GPCP with higher concentration at exterior region but lower ratio at interior region. Coupled with XPS, SEM, TEM, and EELS results, we can conclude that GPCP is composed of graphene/PANi composite sheet.

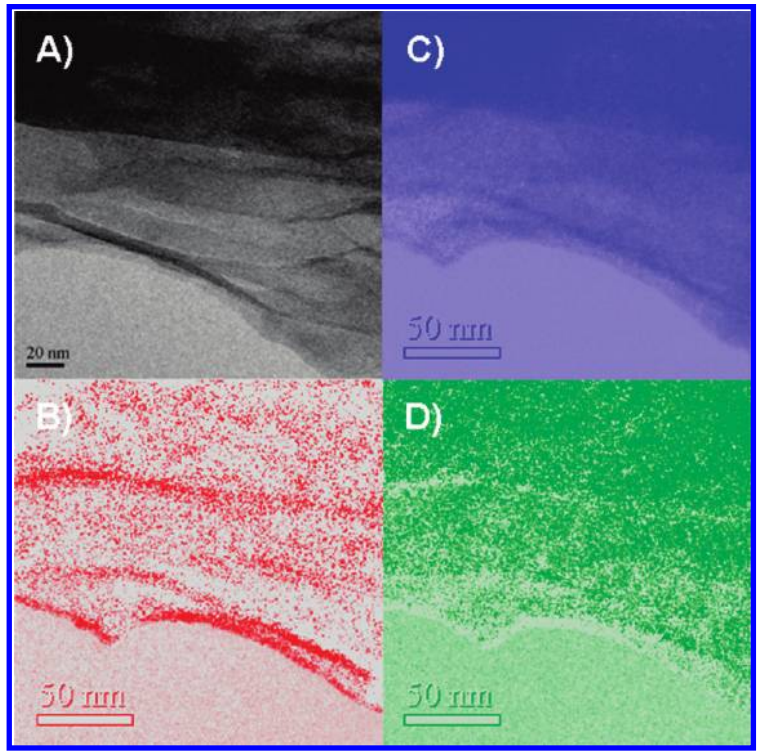


**Figure 7. EELS mapping images of the GPCP-900s: (A) zero-energy loss bright field image, (B) nitrogen element mapping, (C) carbon element mapping, and (D) oxygen element mapping. Note that the images given are not in the exact identical positions due to sample fluctuation but definitely present the information from the same area.**

The mechanical properties of the G-paper and GPCP-900s were measured in SEM by using Gatan *in situ* microtester (200 N). The strain−stress curve of the GPCP-900s reveals a tensile strength of 12.6 MPa with a strain of 0.11, which is better than that of the G-paper (8.8 MPa at 0.08 strain; Figure 8). This result demonstrates the mechanical durability of GPCP-900s as a current-collector-free and binderless free-standing electrode for flexible supercapacitors (inset of Figure 8). The higher tensile strength of GPCP-900s than that of G-paper is due to the enhanced mechanical connection among layered graphene/PANi sheets after AEP treatment. However, we noted that the tensile strength of our G-paper and GPCP-900s is much smaller than that reported for graphene or graphene oxide papers.[16,25,31,32] This is probably due to the differ-

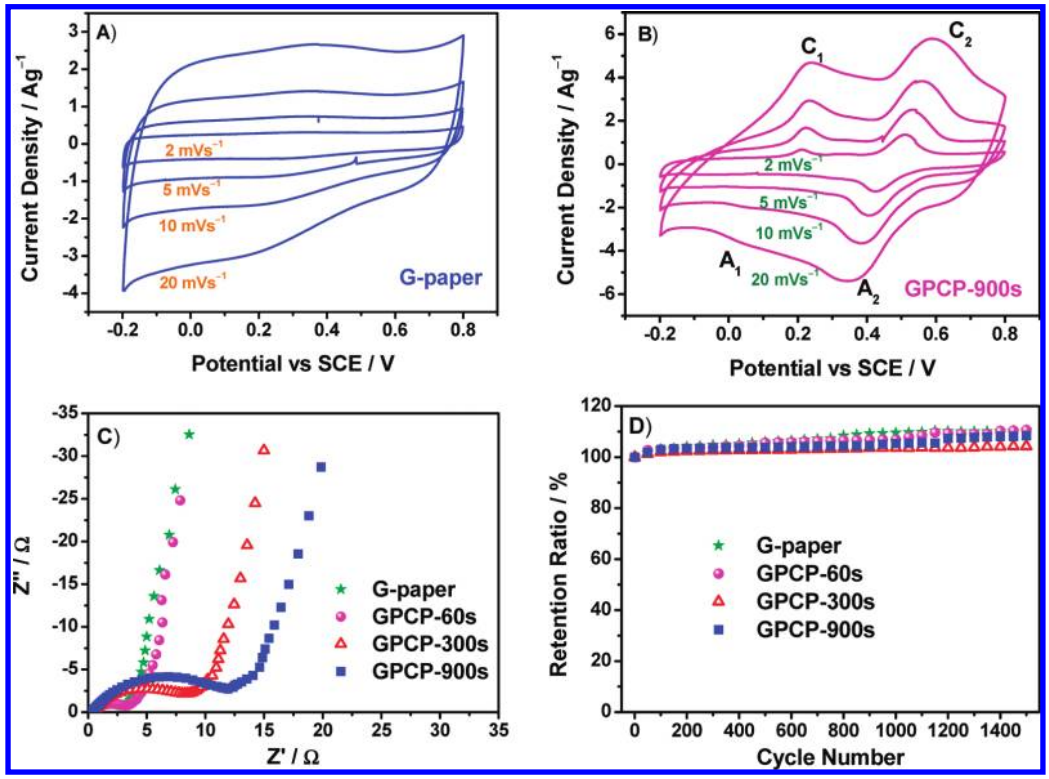


**Figure 9. Electrochemical properties of the G-paper and GPCP. (A,B) Cyclic voltammograms recorded from 2 to 20 mV $s^{-1}$ in 1 M $H_2SO_4$. (C) Nyquist plots of the G-paper and GPCP-60s/300s/900s. (D) Cycling stability measured at 50 mV $s^{-1}$.**

ent structure and properties of graphene and the infiltration conditions for paper formation, where our G-paper and GPCP-900s show porous characteristic (Figure 5A,BB) with a specific surface area of 94 and 39 $m^2\ g^{-1}$, respectively. Further enhancement of the G-paper strength by reducing porosity can be useful to improve the tensile property of GPCP but may probably minimize the electrochemical accessible areas. Therefore, the preparation of an advanced GPCP electrode must require careful balance between the porosity and tensile strength.

Cyclic voltammetry (CV) was run on the G-paper and GPCP-900s in 1 M $H_2SO_4$ electrolyte with a potential window from −0.2 to 0.8 V *versus* SCE. From the cyclic voltammograms shown in Figure 9A,B, the remarkable difference of electrochemical surface activity between the G-paper and GPCP-900s can be easily recognized. The G-paper shows only one pair of redox peaks due to the transition between quinone/hydroquinone groups, which is typical for carbon materials.[40] However, two couples of redox peaks ($C_1/A_1$, $C_2/A_2$) from the GPCP-900s indicate the presence of pseudocapacitive PANi.[34] Redox transitions between a semiconducting state (leucoemeraldine form) and a conducting state (polaronic emeraldine form) are responsible for peaks $C_1/A_1$, and the Faradaic transformation of emeraldine−pernigraniline initiates the redox peaks $C_2/A_2$.[34] It is also noted that the cathodic peaks ($C_1/C_2$) shift positively and the anodic peaks ($A_1/A_2$) shift negatively with the increment of potential sweep rates from 2 to 20 mV $s^{-1}$ (Figure 9B). Impedance measurements can provide useful information about the redox reaction resistance and equivalent series resistance. From the Nyquist plots displayed in Figure 9C, it is apparent that the redox reaction resistance of GPCP increases significantly to 11.64 Ω with the agglomeration of PANi. For the G-paper, the redox reaction resistance for quinone/hydroquinone pair is only 2.72 Ω. On the other hand, the equivalent series resistance of the GPCP (0.36−0.51 Ω) is larger than that of the G-paper (0.28 Ω) because of the lower conductivity of PANi. In addition, the GPCP flexible supercapacitors exhibit good cycling stability (Figure 9D). More importantly, further efforts are necessary to evaluate the relationships between electrochemical stability and mechanical durability because repeated folding may induce performance fading owing to certain structure corruptions.

The gravimetric and volumetric capacitances of the G-paper and GPCP are compared with those of other carbon-based flexible electrodes. The GPCP-900s gave the highest capacitance of 233 F $g^{-1}$, reaching a 58% enhancement in comparison with the G-paper (147 F $g^{-1}$). The gravimetric capacitance of G-paper is very high taking into account its low specific surface area. This should be attributed to the pseudocapacitance of oxygen functional groups, which have a 14 at % concentration according to XPS analysis. It is worth noting that the capacitance of GPCP-900s is larger than that of freestanding electrodes made from one-dimensional carbon nanostructures.[8,9,12,14] We also measured the volumetric

capacitance of the GPCP and G-paper because it is a more important requirement than gravimetric capacitance for flexible supercapacitors. The density of G-paper is 0.44 g $cm^{-3}$, while the density of GPCP ranges 0.51−0.58 g $cm^{-3}$. The GPCP-900s also showed the best performance for volumetric charge storage with a value of 135 F $cm^{-3}$, which is much larger than that of the G-paper (64 F $cm^{-3}$), carbon nanotubes (<16 F $cm^{-3}$),[10,41] carbide-derived carbon (61−90 F $cm^{-3}$),[42] and activated carbons (usually less than 50 F $cm^{-3}$).[41,43] The volumetric capacitance of the G-paper and GPCP is also larger than that of a graphene/binder paste electrode (~53 F $cm^{-3}$).[27] A buckypaper/polyaniline flexible electrode showed a higher gravimetric capacitance than our GPCP-900s.[44] This is probably due to the higher polyaniline ratio in the highly porous buckypaper (70% pore volume), which enables larger accommodation amount of polyaniline. Inspired by this result, our GPCP electrode can be further improved by increasing the porosity.

## CONCLUSIONS

In summary, a combination of flow-directed assembly and *in situ* anodic electropolymerization techniques was used to fabricate graphene/polyaniline composite paper with favorable flexibility and electrochemical activity. The GPCP retains the layer-by-layer structure of the G-paper and exhibits an improved mechanical tensile strength (by 43%) and electrochemical capacitance (by maximum 58%). The unique graphene/PANi composite sheets in GPCP offer an enhanced electron transfer from graphene to highly active PANi film and act as tensile backbones to maintain a desirable mechanical flexibility. The greatest gravimetric and volumetric capacitances of the GPCP-900s reach 233 F $g^{-1}$ and 135 F $cm^{-3}$, respectively, much larger than those of the G-paper (147 F $g^{-1}$ and 64 F $cm^{-3}$) and many other currently available carbon-based flexible electrodes. These intriguing features make it quite a promising material as a freestanding electrode for flexible supercapacitors. Furthermore, the results are also potentially useful for the preparation of other graphene-based composite papers with varied properties in order to meet diverse applications in flexible lithium ion batteries, chemical sensors, solar cells, *etc*.

## EXPERIMENTAL SECTION

**Synthesis of the G-Paper:** Graphene was prepared from natural flake graphite powder (Sinopharm Chemical Reagent Co., Ltd.), as reported elsewhere.[45] Four steps were involved in the G-paper preparation: (i) oxidation of the starting natural flake graphite powder to prepare graphite oxide (GO) using Hummers method; (ii) fast thermal expansion/exfoliation of GO (1050 °C, Ar, 30 s) to synthesize thermally expanded graphite oxide (TEGO); (iii) hydrogen reduction of TEGO (400 °C, 2 h) and dispersion/high-speed centrifugation of reduced TEGO to obtain a graphene suspension; (iv) filtration of the graphene suspension through a membrane to fabricate the G-paper, followed by vacuum drying at 80 °C.

**Synthesis of the GPCP:** The three-electrode AEP cell was constructed with a Pt plate as counter electrode and SCE as reference electrode. G-paper was directly used as the working electrode. The electrolyte was 0.5 M $H_2SO_4$ and 0.05 M aniline. PANi was *in situ* electropolymerized on the G-paper at a constant potential of 0.75 V *versus* SCE for different periods (60, 300, and 900 s). After electropolymerization, the GPCP was washed with distilled water and dried.

**Characterizations of the G-Paper and GPCP:** Raman spectra were recorded using micro-Raman spectroscopy (Jobin Yvon LabRam HR800, excited by 632.8 nm He−Ne laser) to monitor the surface composition of the G-paper and GPCP. The morphology and structure of the G-paper and GPCP were characterized by SEM (FEI Nova NanoSEM 430, 15 kV), TEM (JEOL JEM-2010, 200 kV), and EELS mapping (FEI Tecnai F30, 300 kV). Mechanical measurements were conducted in an SEM with Gatan *in situ* microtest (200 N). Specific surface area was determined using Micromeritics ASAP 2010 M instrument at liquid nitrogen temperature. XPS analysis was performed on ESCALAB 250 instrument with Al Kα radiation (15 kV, 150 W) under a pressure of $4 \times 10^{-8}$ Pa.

**Electrochemical Measurement of the G-Paper and GPCP:** The G-paper and GPCP were directly used as electrodes in a three-electrode test cell with 1 M $H_2SO_4$ electrolyte. The thicknesses of the electrodes of G-paper, GPCP-60s, GPCP-300s, and GPCP-900s are 102, 90, 90, and 104 μm, respectively. The cyclic voltammograms were collected on Solartron 1287 electrochemical instrument from 2 to 20 mV $s^{-1}$. The CV potential range was −0.2 to 0.8 V *versus* SCE in $H_2SO_4$ electrolyte with a Pt plate as counter electrode. Electrochemical impedance spectra were recorded using Solartron 1260 from 10 mHz to 10 kHz with an alternate current amplitude of 10 mV. The cycle stability of the electrodes was determined in cells after evacuating dissolved air. The gravimetric capacitance of the electrodes was calculated according to $C_g = (\int i dV)/(\nu m V)$, where $i$ is the current density during charging or discharging, $V$ is the potential, $\nu$ is the potential sweep rate, and $m$ is the mass of the paper electrodes. The volumetric capacitance was calculated by dividing the gravimetric capacitance with the apparent density of the paper electrodes.

*Acknowledgment.* The authors acknowledge financial support from NSFC grants (No. 50872136, No. 50632040, and No. 90606008), MOST of China (No. 2006CB932703), and Chinese Academy of Sciences (No. KJCX2-YW-M01).

*Note added after ASAP publication:* In the version of this article published June 2, 2009, an incorrect unit of measure appeared on the first page; 7200 S $cm^{-1}$ should have read 7200 S $m^{-1}$. The corrected article reposted June 5, 2009.

## REFERENCES AND NOTES

1. Sugimoto, W.; Yokoshima, K.; Ohuchi, K.; Murakami, Y.; Takasu, Y. Fabrication of Thin-Film, Flexible, and Transparent Electrodes Composed of Ruthenic Acid Nanosheets by Electrophoretic Deposition and Application to Electrochemical Capacitors. *J. Electrochem. Soc.* **2006**, *153*, A255–A260.
2. Pushparaj, V. L.; Shaijumon, M. M.; Kumar, A.; Murugesan, S.; Ci, L.; Vajtai, R.; Linhardt, R. J.; Nalamasu, O.; Ajayan, P. M. Flexible Energy Storage Devices Based on Nanocomposite Paper. *Proc. Natl. Acad. Sci. U.S.A.* **2007**, *104*, 13574–13577.
3. Nam, K. T.; Kim, D. W.; Yoo, P. J.; Chiang, C. Y.; Meethong, N.; Hammond, P. T.; Chiang, Y. M.; Belcher, A. M. Virus-Enabled Synthesis and Assembly of Nanowires for Lithium Ion Battery Electrodes. *Science* **2006**, *312*, 885–888.
4. Lu, X. M.; Xia, Y. N. Electronic Materials: Buckling down for Flexible Electronics. *Nat. Nanotechnol.* **2006**, *1*, 163–164.
5. Sun, Y. G.; Rogers, J. A. Inorganic Semiconductors for Flexible Electronics. *Adv. Mater.* **2007**, *19*, 1897–1916.

6. Kim, D. H.; Ahn, J. H.; Choi, W. M.; Kim, H. S.; Kim, T. H.; Song, J. Z.; Huang, Y. G. Y.; Liu, Z. J.; Lu, C.; Rogers, J. A. Stretchable and Foldable Silicon Integrated Circuits. *Science* **2008**, *320*, 507–511.
7. Conway, B. E. *Electrochemical Supercapacitors: Scientific Fundamentals and Technological Applications*; Plenum Publishers: New York, 1999.
8. Kim, C.; Choi, Y. O.; Lee, W. J.; Yang, K. S. Supercapacitor Performances of Activated Carbon Fiber Webs Prepared by Electrospinning of PMDA-ODA Poly(amic acid) Solutions. *Electrochim. Acta* **2004**, *50*, 883–887.
9. Beguin, F.; Szostak, K.; Lota, G.; Frackowiak, E. A Self-Supporting Electrode for Supercapacitors Prepared by One-Step Pyrolysis of Carbon Nanotube/Polyacrylonitrile Blends. *Adv. Mater.* **2005**, *17*, 2380–2384.
10. Futaba, D. N.; Hata, K.; Yamada, T.; Hiraoka, T.; Hayamizu, Y.; Kakudate, Y.; Tanaike, O.; Hatori, H.; Yumura, M.; Iijima, S. Shape-Engineerable and Highly Densely Packed Single-Walled Carbon Nanotubes and Their Application as Supercapacitor Electrodes. *Nat. Mater.* **2006**, *5*, 987–994.
11. Kaempgen, M.; Ma, J.; Gruner, G.; Wee, G.; Mhaisalkar, S. G. Bifunctional Carbon Nanotube Networks for Supercapacitors. *Appl. Phys. Lett.* **2007**, *90*, 264104.
12. Ci, L. J.; Manikoth, S. M.; Li, X. S.; Vajtai, R.; Ajayan, P. M. Ultrathick Freestanding Aligned Carbon Nanotube Films. *Adv. Mater.* **2007**, *19*, 3300–3303.
13. Chen, J.; Minett, A. I.; Liu, Y.; Lynam, C.; Sherrell, P.; Wang, C.; Wallace, G. G. Direct Growth of Flexible Carbon Nanotube Electrodes. *Adv. Mater.* **2008**, *20*, 566–570.
14. Choua, S. L.; Wang, J. Z.; Chewa, S. Y.; Liua, H. K.; Doua, S. X. Electrodeposition of $MnO_2$ Nanowires on Carbon Nanotube Paper as Free-Standing, Flexible Electrode for Supercapacitors. *Electrochem. Commun.* **2008**, *10*, 1724–1727.
15. Stankovich, S.; Dikin, D. A.; Dommett, G. H. B.; Kohlhaas, K. M.; Zimney, E. J.; Stach, E. A.; Piner, R. D.; Nguyen, S. T.; Ruoff, R. S. Graphene-Based Composite Materials. *Nature* **2006**, *442*, 282–286.
16. Dikin, D. A.; Stankovich, S.; Zimney, E. J.; Piner, R. D.; Dommett, G. H. B.; Evmenenko, G.; Nguyen, S. T.; Ruoff, R. S. Preparation and Characterization of Graphene Oxide Paper. *Nature* **2007**, *448*, 457–460.
17. Bunch, J. S.; van der Zande, A. M.; Verbridge, S. S.; Frank, I. W.; Tanenbaum, D. M.; Parpia, J. M.; Craighead, H. G.; McEuen, P. L. Electromechanical Resonators from Graphene Sheets. *Science* **2007**, *315*, 490–493.
18. Watcharotone, S.; Dikin, D. A.; Stankovich, S.; Piner, R.; Jung, I.; Dommett, G. H. B.; Evmenenko, G.; Wu, S. E.; Chen, S. F.; Liu, C. P.; Nguyen, S. T.; Ruoff, R. S. Graphene−Silica Composite Thin Films as Transparent Conductors. *Nano Lett.* **2007**, *7*, 1888–1892.
19. Gomez-Navarro, C.; Weitz, R. T.; Bittner, A. M.; Scolari, M.; Mews, A.; Burghard, M.; Kern, K. Electronic Transport Properties of Individual Chemically Reduced Graphene Oxide Sheets. *Nano Lett.* **2007**, *7*, 3499–3503.
20. Schedin, F.; Geim, A. K.; Morozov, S. V.; Hill, E. W.; Blake, P.; Katsnelson, M. I.; Novoselov, K. S. Detection of Individual Gas Molecules Adsorbed on Graphene. *Nat. Mater.* **2007**, *6*, 652–655.
21. Ramanathan, T.; Abdala, A. A.; Stankovich, S.; Dikin, D. A.; Herrera-Alonso, M.; Piner, R. D.; Adamson, D. H.; Schniepp, H. C.; Chen, X.; Ruoff, R. S.; Nguyen, S. T.; Aksay, I. A.; Prud'homme, R. K.; Brinson, L. C. Functionalized Graphene Sheets for Polymer Nanocomposites. *Nat. Nanotechnol.* **2008**, *3*, 327–331.
22. Balandin, A. A.; Ghosh, S.; Bao, W. Z.; Calizo, I.; Teweldebrhan, D.; Miao, F.; Lau, C. N. Superior Thermal Conductivity of Single-Layer Graphene. *Nano Lett.* **2008**, *8*, 902–907.
23. Gomez-Navarro, C.; Burghard, M.; Kern, K. Elastic Properties of Chemically Derived Single Graphene Sheets. *Nano Lett.* **2008**, *8*, 2045–2049.
24. Wang, X.; Zhi, L. J.; Mullen, K. Transparent, Conductive Graphene Electrodes for Dye-Sensitized Solar Cells. *Nano Lett.* **2008**, *8*, 323–327.
25. Li, D.; Muller, M. B.; Gilje, S.; Kaner, R. B.; Wallace, G. G. Processable Aqueous Dispersions of Graphene Nanosheets. *Nat. Nanotechnol.* **2008**, *3*, 101–105.
26. Yoo, E.; Kim, J.; Hosono, E.; Zhou, H.; Kudo, T.; Honma, I. Large Reversible Li Storage of Graphene Nanosheet Families for Use in Rechargeable Lithium Ion Batteries. *Nano Lett.* **2008**, *8*, 2277–2282.
27. Stoller, M. D.; Park, S. J.; Zhu, Y. W.; An, J. H.; Ruoff, R. S. Graphene-Based Ultracapacitors. *Nano Lett.* **2008**, *8*, 3498–3502.
28. Vivekchand, S. R. C.; Rout, C. S.; Subrahmanyam, K. S.; Govindaraj, A.; Rao, C. N. R. Graphene-Based Electrochemical Supercapacitors. *J. Chem. Sci.* **2008**, *120*, 9–13.
29. Subrahmanyam, K. S.; Vivekchand, S. R. C.; Govindaraj, A.; Rao, C. N. R. A Study of Graphenes Prepared by Different Methods: Characterization, Properties and Solubilization. *J. Mater. Chem.* **2008**, *18*, 1517–1523.
30. Paek, S. M.; Yoo, E.; Honma, I. Enhanced Cyclic Performance and Lithium Storage Capacity of $SnO_2$/Graphene Nanoporous Electrodes with Three-Dimensionally Delaminated Flexible Structure. *Nano Lett.* **2009**, *9*, 72–75.
31. Chen, H.; Muller, M. B.; Gilmore, K. J.; Wallace, G. G.; Li, D. Mechanically Strong, Electrically Conductive, and Biocompatible Graphene Paper. *Adv. Mater.* **2008**, *20*, 3557–3561.
32. Xu, Y. X.; Bai, H.; Lu, G. W.; Li, C.; Shi, G. Q. Flexible Graphene Films *via* the Filtration of Water-Soluble Noncovalent Functionalized Graphene Sheets. *J. Am. Chem. Soc.* **2008**, *130*, 5856–5857.
33. Jang, J. Conducting Polymer Nanomaterials and Their Applications. *Adv. Polym. Sci.* **2006**, *199*, 189–259.
34. Wang, Y. G.; Li, H. Q.; Xia, Y. Y. Ordered Whiskerlike Polyaniline Grown on the Surface of Mesoporous Carbon and its Electrochemical Capacitance Performance. *Adv. Mater.* **2006**, *18*, 2619–2623.
35. Fan, L. Z.; Hu, Y. S.; Maier, J.; Adelhelm, P.; Smarsly, B.; Antonietti, M. High Electroactivity of Polyaniline in Supercapacitors by Using a Hierarchically Porous Carbon Monolith as a Support. *Adv. Funct. Mater.* **2007**, *17*, 3083–3087.
36. Bernard, M. C.; Goff, A. H. L. Quantitative Characterization of Polyaniline Films Using Raman Spectroscopy I: Polaron Lattice and Bipolaron. *Electrochim. Acta* **2006**, *52*, 595–603.
37. Bernard, M. C.; Goff, A. H. L.; Arkoub, H.; Saidani, B. Characterization of Substituted Polyaniline Films Using Raman Spectroscopy. III. Study of a Methoxylated Polymer POMA. *Electrochim. Acta* **2007**, *52*, 5030–5038.
38. Bernard, M. C.; Goff, A. H. L. Quantitative Characterization of Polyaniline Films Using Raman Spectroscopy II. Effects of Self-Doping in Sulfonated Polyaniline. *Electrochim. Acta* **2006**, *52*, 728–735.
39. Efremova, A.; Regis, A.; Arsov, L. Electrochemical Formation and Deposition of Polyaniline on Electrode Surface: *In-Situ* Raman Spectroscopical Study. *Electrochim. Acta* **1994**, *39*, 839–845.
40. Nian, Y. R.; Teng, H. S. Nitric acid Modification of Activated Carbon Electrodes for Improvement of Electrochemical Capacitance. *J. Electrochem. Soc.* **2002**, *149*, A1008–A1014.
41. Emmenegger, C.; Mauron, P.; Sudan, P.; Wenger, P.; Hermann, V.; Gallay, R.; Zuttel, A. Investigation of Electrochemical Double-Layer (ECDL) Capacitors Electrodes Based on Carbon Nanotubes and Activated Carbon Materials. *J. Power Sources* **2003**, *124*, 321–329.
42. Fernandez, J. A.; Arulepp, M.; Leis, J.; Stoeckli, F.; Centeno, T. A. EDLC Performance of Carbide-Derived Carbons in Aprotic and Acidic Electrolytes. *Electrochim. Acta* **2008**, *53*, 7111–7116.
43. Kim, Y. J.; Abe, Y.; Yanaglura, T.; Park, K. C.; Shimizu, M.; Iwazaki, T.; Nakagawa, S.; Endo, M.; Dresselhaus, M. S. Easy Preparation of Nitrogen-Enriched Carbon Materials from Peptides of Silk Fibroins and Their Use to Produce a High Volumetric Energy Density in Supercapacitors. *Carbon* **2007**, *45*, 2116–2125.

44. Meng, C.; Liu, C.; Fan, S. Flexible Carbon Nanotube/Polyaniline Paper-like Films and Their Enhanced Electrochemical Properties. *Electrochem. Commun.* **2009**, *11*, 186–189.
45. Wu, Z. S.; Ren, W.; Gao, L.; Jiang, C.; Cheng, H. M. Synthesis of High-Quality Graphene with a Predetermined Number of Layers. *Carbon* **2009**, *47*, 493–499.